34th Annual International Conference of the IEEE EMBS
San Diego, California USA, 28 August - 1 September, 2012

Timing Detection and Seismocardiography Waveform Extraction

Hoang Nguyen,[1] Jianzhong (Charlie) Zhang,[2] and Young-Han Nam[3]
Dallas Technology Lab, Samsung Electronics
Richardson, Texas, USA

Abstract— **Described herein is a new and robust method to extract heart-beat timing from seismocardiogram (SCG). This timing indicates the precise time location of each heart beat and therefore directly conveys heart rate information. Knowledge of the time location of each occurrence of the underlying SCG waveform allows us to obtain a clean SCG waveform estimate by time averaging noisy segments of an SCG time series. The algorithm can be implemented in wearable SCG-based devices to provide heart monitoring or diagnosis capabilities without relying on any other methodology, such as electrocardiography, as a timing reference.**

I. Introduction

Seismocardiography is a technique for measuring and analyzing the heart's activity manifested in the form of mechanical vibrations. The most commonly used measure is the vibrational acceleration detected by an accelerometer placed on the outer chest wall. It has been found [1], [2] that well-defined events in the cardiac cycle can be identified on the seismocardiogram (SCG). Furthermore, the SCG waveform and particularly its morphology contains information about the heart's health. A reasonably comprehensive study of the effectiveness of SCG in detecting coronary artery disease (CAD) is given in [3]. Also, SCG has been used as a noninvasive means to study myocardial contractility under hyperbaric exposure [4]. A variant of SCG called quantitative ballistocardiogram has been used to study systolic force in relation to ageing [5].

Although SCG came into existence many decades ago, its potential benefits have been unexplored commercially, in part due to lack of simple sensors and signal processing methods that can reliably extract information. With the advancement of MEMS-based sensors and low-power microprocessors, interests have recently increased in small-size and light-weight systems for capturing and processing of SCG to provide continuous heart monitoring [6]–[8]. With further research and development, SCG may find its way into consumer electronics to provide advanced health and life care capabilities such as noninvasive heart disease detection.

Past studies on SCG, however, were conducted not with SCG alone but with the assistance of an electrocardiogram (ECG) as a timing reference [1], [8]–[10]. The work of [8] in particular uses the ECG timing reference to obtain a clean SCG waveform, from which the so-called the I-J index can be extracted that provides an estimate of the cardiac output.

[1,2,3] Emails: hnguyen2@sta.samsung.com, jzhang@sta.samsung.com, ynam@sta.samsung.com.

A common component of many existing approaches to SCG processing and information extraction is the use of the ECG as a timing reference. While SCG has potential benefits over ECG such as better sensitivity and specificity in detecting CAD [3], a device's reliance on ECG would marginalize these benefits because ECG is well understood and can by itself provide most if not all the information that the SCG can. From the commercial and user-convenience viewpoint, it is highly desirable to have a device or system that can extract as much or more information from the SCG without ECG. Furthermore, unlike ECG, SCG has an added advantage that it is magnetically compatible, i.e., it can be obtained with sensors immune to magnetic interference. Magnetic compatibility makes SCG a potentially useful tool for removing vibration-induced impairments from MRI [11], [12].

The ability to reliably extract timing information from the SCG alone is therefore desirable. In particular, a clean SCG waveform of a cardiac cycle (heart beat) is necessary for SCG-based diagnoses. This problem has received little attention, but there is a method in [13] which uses the time widths of the raising edges in the SCG time series to detect what is called the pseudo-period, that is the main swing of the SCG waveform of a cardiac cycle; more specifically, the main swing occurs in the systolic complex (contraction phase) of each cardiac cycle. The method assumes that the main swing's duration remains constant for different heart beats. This approach seems to work reasonably well for a clean SCG record, but we seek a more robust algorithm in order to deal with poor-quality SCG data obtained from low-cost MEMS-based accelerometers, subject to various sources of interference and noise.

In this paper we propose a robust method to extract the timing from the SCG alone. This timing directly conveys heart rate information. The precise time location of each occurrence of the SCG waveform allows us to obtain a clean SCG waveform estimate by time averaging noisy SCG segments identified by the timing locations.

II. Signal Model and Algorithms

A. Signal modeling

It has been determined that resting seismocardiogram is stable over a period of at least 3 months [1]. Assuming a perfect accelerometer affixed to a given point on the outer chest wall of a given person, the sensor response in a given direction to any isolated heart beat can be represented as a

function of time $s(t), t \in [0, \infty)$. By the resting SCG being stable means that $s(t)$ is the same for all resting heart beats within a typical measurement time interval (e.g., minutes long). As the heart continues to beat, by superposition the sensor response traces out a time series

$$x(t) = \sum_{k=0}^{\infty} s(t - t_k) \,, \tag{2.1}$$

where t_k represents the start time of the kth beat, with $t_k < t_{k+1}$. Here, the term "start time" of a heart beat need not be defined precisely, but it's sufficient for our purpose to define it as some point shortly before the main swing of the SCG, such as the time point of the P-peak [3] of the ECG. The time between two consecutive beats is not constant and appears somewhat random from beat to beat, so t_k is not known.

Although acceleration is an analog quantity, it can be assumed to have finite spectral bandwidth in practice. With a sufficiently high sampling rate, it can be converted to a discrete-time process without loss of information. Therefore, we only deal with discrete-time processes in this paper.

Because each heart beat delivers a finite energy, $s(t)$ has finite energy, i.e., $\sum_{t=0}^{\infty} s^2(t) < \infty$. Actual SCG data suggests that practically all the energy of $s(t)$ is contained within a time interval $[0, L)$ shorter than the time between consecutive heart beats. This is manifested by the fact that a clean SCG time series shows clear repetitions of the same waveform over time such that the heart beats can be visually identified.

Existing works indicate that the SCG waveform $s(t)$ contains information that can be used to perform diagnoses such as CAD detection [3] or give certain indicator such as the cardiac output [8]. Much of the information is carried in the morphology of the SCG waveform and therefore having a clean SCG waveform is crucial to the reliability of such diagnoses and indicators. However, obtaining a clean SCG waveform directly from an accelerometer is not practical, because sensor responses are inherently noisy, and measurements are subject to interferences due to the subject's movements, breathing and heart noises. With impairments, the data can be modeled as

$$r(t) = x(t) + w(t) \,, \tag{2.2}$$

where $w(t)$ represents the combination of all impairments and is treated as a random process.

Given only the observation $r(t)$ in some finite time interval $[0, N-1]$, we seek a reliable estimate of the SCG waveform. To achieve this, we propose to find the starting time location of each occurrence of $s(t)$ in the record of $r(t)$, and then perform time averaging to suppress the interferences and noises. Specifically, for each $k = 1, 2, ..., \nu$, we first determine t_k, i.e., the starting time of the k-th beat to construct a length-L time series comprising L consecutive time samples of $r(t)$ starting from $t = t_k$; and obtain an estimate of $s(t)$ as

$$\bar{s}(t) = \frac{1}{\nu} \sum_{k=1}^{\nu} r(t + t_k) \,, t = 0, 1, 2, ..., L-1, \tag{2.3}$$

assuming $w(t)$ is a zero-mean uncorrelated process.

B. Timing detection

Given an N-sample observation record $\{r(t)\}_{t=0}^{N-1}$, timing can be determined as follows. Define the vectors

$$\mathbf{r}(k) \triangleq [r(k), r(k+1), ..., r(k+L-1)]^T \tag{2.4}$$

$$\mathbf{w}(k) \triangleq [w(k), w(k+1), ..., w(k+L-1)]^T \,. \tag{2.5}$$

The basic idea employed here is to use $\mathbf{r}(\tau)$, with some fixed τ, as a reference and then perform hypothesis testing to discriminate between $\mathbf{r}(\tau)$ and $\mathbf{r}(k)$ for $k = 0, 1, ..., N-1$. For any fixed $\tau \in \{0, 1, ..., N-1\}$, there is an i such that $t_i \leq \tau < t_{i+1}$, i.e., $\tau = t_i + d < t_{i+1}$ with $d \geq 0$. With the assumption of no inter-beat interference,

$$\mathbf{r}(\tau) = \mathbf{s} + \mathbf{w}(\tau) \tag{2.6}$$

where $\mathbf{s}$ contains samples from the vector

$$\mathbf{s}^{(i)} \triangleq [s(0), s(1), ..., s(t_{i+1} - t_i - 1)]^T \,. \tag{2.7}$$

More specifically, if $t_i + d + L - 1 < t_{i+1}$, then $\mathbf{s} = [s(d), s(d+1), ..., s(d+L-1)]^T$. Otherwise, $\mathbf{s} = [s(d), s(d+1), ..., s(t_{i+1} - t_i - 1), s(0), s(1), ..., s(t_i + d + L - t_{i+1} - 1)]^T$. The choice of τ is not crucial, but it should be chosen such that $\mathbf{r}(\tau)$ captures most of the energy of $s(t)$, e.g., $||\mathbf{r}(\tau)||^2$ is maximum.

Now, if $k = t_j + d$ for some j and the same d as above, then $\mathbf{r}(k) = \mathbf{s} + \mathbf{w}(k)$. That is, $\mathbf{r}(\tau)$ and $\mathbf{r}(k)$ in this case are noisy versions of the same underlying signal $\mathbf{s}$, and therefore $\tau + t$ and $k + t$ $(0 \leq t < L)$ mark the same point in the cardiac cycle but lie in two different heart beats. From this insight, we decide for each k whether $\mathbf{r}(k)$ matches $\mathbf{r}(\tau)$ by testing the hypothesis H_1 against H_0, where

$$H_1 : \mathbf{r}(\tau) = \mathbf{s} + \mathbf{w}(\tau) \tag{2.8}$$

$$\mathbf{r}(k) = \mathbf{s} + \mathbf{w}(k) \tag{2.9}$$

$$H_0 : \mathbf{r}(\tau) = \mathbf{s} + \mathbf{w}(\tau) \tag{2.10}$$

$$\mathbf{r}(k) = \tilde{\mathbf{s}} + \mathbf{w}(k) \tag{2.11}$$

with $\tilde{\mathbf{s}}$ consisting of samples from a different interval of the SCG waveform than the interval for $\mathbf{s}$. For simplicity, we assume that $\mathbf{w}(\tau)$ and $\mathbf{w}(k)$ are uncorrelated and admit the Gaussian distribution $N(\underline{0}, N_0 \mathbf{I}_L)$, where $\mathbf{I}_L$ denotes the $L \times L$ identity matrix. Note that $\mathbf{s}$, $\tilde{\mathbf{s}}$ and N_0 are all unknown. Although hypothesis H_0 as defined by (2.10) and (2.11) comes directly from our basic signal model (2.1), it is unwieldy because it does not allow for easy estimation of all the unknowns $\mathbf{s}$, $\tilde{\mathbf{s}}$ and N_0 simultaneously. However, because $\tilde{\mathbf{s}}$ and $\mathbf{s}$ are different, the correlation between $\mathbf{r}(\tau)$ and $\mathbf{r}(k)$ under H_0 is weak and therefore, we treat them as uncorrelated Gaussian vectors by adopting the model

$$H_0 : \mathbf{r}(\tau) = \mathbf{w}(\tau) \tag{2.12}$$

$$\mathbf{r}(k) = \mathbf{w}(k) \tag{2.13}$$

$$\mathbf{w}(\tau), \mathbf{w}(k) \sim N(\underline{0}, N_0 \mathbf{I}_L) \,. \tag{2.14}$$

Depending on the hypothesis, the maximum-likelihood (ML) estimates for N_0 and $\mathbf{s}$ are differently obtained. Under H_1,

the ML estimates for $\mathbf{s}$ and N_0 respectively are

$$\hat{\mathbf{s}} = \frac{\mathbf{r}(\tau) + \mathbf{r}(k)}{2} \tag{2.15}$$

$$\hat{N_0} = \frac{||\mathbf{r}(\tau) - \mathbf{r}(k)||^2}{4L} \,. \tag{2.16}$$

Under H_0 as defined by (2.12)–(2.14), the ML estimate for N_0 is

$$\tilde{N_0} = \frac{||\mathbf{r}(\tau)||^2 + ||\mathbf{r}(k)||^2}{2L} \,. \tag{2.17}$$

The generalized likelihood ratio (GLR) of H_1 over H_0 is defined as

$$\Lambda(k;\tau) \stackrel{\triangle}{=} \frac{f(\mathbf{r}(\tau), \mathbf{r}(k) | \mathbf{s} = \hat{\mathbf{s}}, N_0 = \hat{N_0}, H_1)}{f(\mathbf{r}(\tau), \mathbf{r}(k) | N_0 = \tilde{N_0}, H_0)} \tag{2.18}$$

$$= \frac{2^L (||\mathbf{r}(\tau)||^2 + ||\mathbf{r}(k)||^2)^L}{(||\mathbf{r}(\tau) - \mathbf{r}(k)||^2)^L} \,. \tag{2.19}$$

where $f(\mathbf{r}(\tau), \mathbf{r}(k) | \mathbf{s} = \hat{\mathbf{s}}, N_0 = \hat{N_0}, H_1)$ is the probability density of $(\mathbf{r}(\tau), \mathbf{r}(k))$ with the unknowns being replaced by their respective estimate under H_1. Similarly, $f(\mathbf{r}(\tau), \mathbf{r}(k) | N_0 = \tilde{N_0}, H_0)$ is the probability density of $(\mathbf{r}(\tau), \mathbf{r}(k))$ where the unknown N_0 is replaced by its estimate under H_0. We define the root GLR as

$$R(k;\tau) \stackrel{\triangle}{=} \frac{1}{2}(\Lambda(k;\tau))^{1/L} = \frac{||\mathbf{r}(\tau)||^2 + ||\mathbf{r}(k)||^2}{||\mathbf{r}(\tau) - \mathbf{r}(k)||^2} \,. \tag{2.20}$$

To find the values of k at which it is decided that $\mathbf{r}(k)$ closely aligns with $\mathbf{r}(\tau)$, we define the function

$$Q(k;\tau) \stackrel{\triangle}{=} \begin{cases} R(k;\tau), & R(k;\tau) > R_{\mathrm{t}} \\ 0, & \text{otherwise} \end{cases} \tag{2.21}$$

for some threshold R_{t}. A timing match is declared at $k = k_i$ if and only if $Q(k_i;\tau) - Q(k_i - 1;\tau) > 0$ and $Q(k_i + 1;\tau) - Q(k_i;\tau) < 0$; basically k_i is the location of a local peak above R_{t}. Empirical data shows that $R_{\mathrm{t}} = 1.5$ provides good discrimination [see Fig. 3(a), where each k_i locates a sharp peak indicated by a circle]. Note that $R(\tau;\tau) = \infty$.

Accelerometers typically provide data in three orthogonal directions (x, y and z axes) to represent the complete acceleration vector. The algorithm above can be extended to use the data from all three axes. To do so, (2.4) is redefined as

$$\mathbf{r}(k) \stackrel{\triangle}{=} [\mathbf{r}_x^T(k), \mathbf{r}_y^T(k), \mathbf{r}_z^T(k)]^T \tag{2.22}$$

$$\mathbf{r}_v(k) \stackrel{\triangle}{=} [r_v(k), r_v(k+1), ..., r_v(k+L-1)]^T \tag{2.23}$$

where $v \in \{x, y, z\}$ and $r_v(k)$ is the sensor response in direction v. If timing matches are declared at $k = k_1, k_2, ..., k_\nu$, the ML estimate of $\mathbf{s}$ based on the data at the timing matches is given by

$$\bar{\mathbf{s}} = \frac{1}{\nu} \sum_{i=1}^{\nu} \mathbf{r}(k_i) \,. \tag{2.24}$$

It is of practical interest to minimize the computational complexity. One part of this optimization is to avoid computing the GLR at unnecessary times. As soon as a timing match is declared at $k = k_i$, all computations can be skipped at $k = k_i + 2, k_i + 3, ..., k_i + M$, where M is some conservative estimate of the inter-beat time. Computations are resumed at $k_i + M + 1$ until the next timing match k_{i+1} is declared. The process is repeated and can be done in real time.

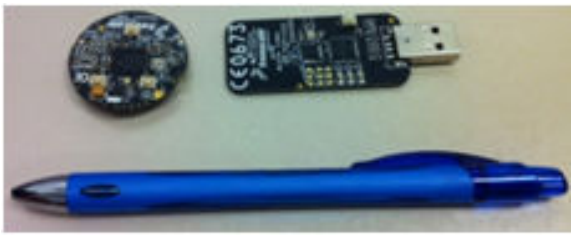

Fig. 1: Picture of the SCG sensor used for the experiment

III. Numerical results and conclusion

To test the algorithm described above, we apply it to a data record obtained by measuring the heart activity of a volunteer. The measurement device used is the 3-axis digital accelerometer MMA8451Q made by Freescale Semiconductor shown in Fig. 1. The sensor is placed such that the z-axis is approximately perpendicular to the volunteer's chest wall. The sampling rate is set at 200 samples per second.

Shown in Fig. 2 is the sensor response in the z-direction. The responses for the x and y directions are similar to that for the z direction and are omitted from this figure to save space. We note that the sensor response in each direction tends to have a linear trend over time, including a nonzero mean due to imperfect calibration. A preprocessing step can be done to remove the linear trend by applying a linear least-squares fit.

Fig. 3 shows the results obtained by applying the algorithm to the preprocessed data. Part (a) shows the root GLR for each time index; sharp peaks arise at indices that indicate timing matches. The vector length used is $L = 200$ and the decision threshold is $R_{\mathrm{t}} = 1.5$. Shown in parts (b), (c) and (d) are the estimated SCG waveforms for the x, y and z directions, respectively, obtained by averaging according to (2.24). The estimated SCG waveforms exhibit a typical morphology.

In conclusion, the GLRT based algorithm is robust and able to definitively decide between presence or absence of a timing match at each time step. The heart rate can be directly computed from the rate of occurrence of timing matches. Once an estimated SCG waveform $\bar{\mathbf{s}}$ is available, it can be used in place of the reference segment $\mathbf{r}(\tau)$ in (2.8)-(2.13) to improve the discrimination performance on future data, such as in applications with live data feeds. One note of caution is that although the method can provide a good estimate for the SCG waveform, it does not guarantee that the estimate is free of influences that consistently alter the sensor response. For example, the manner in which the sensor is attached to the chest, such as the amount of pressure applied to create a sufficiently firm contact between the chest wall and the sensor, can affect the response waveform. This may be important for morphology based diagnoses and warrants further study.

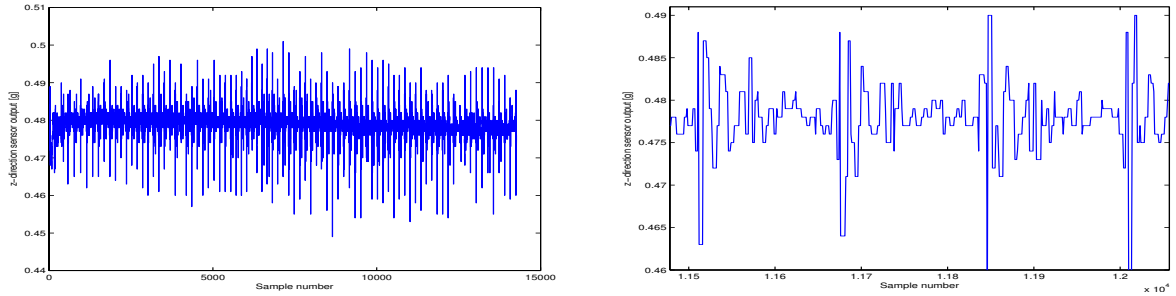

(a) (b)

Fig. 2: (a) Accelerator response in the z-direction while the subject sat still and held its breath. (b) a close-up view of (a).

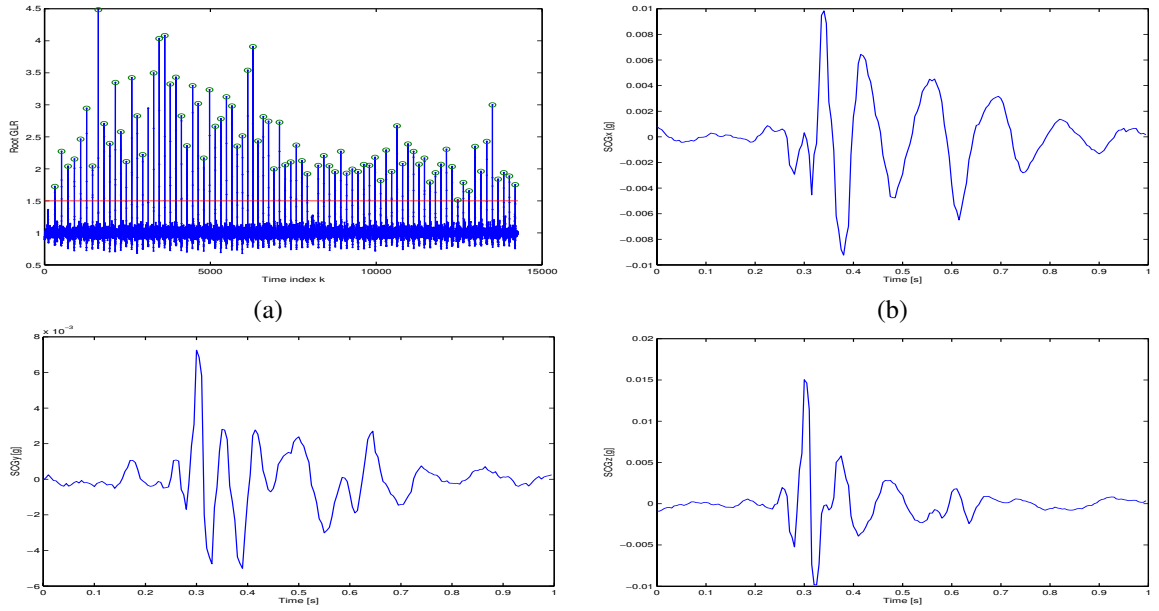

(a) (b) (c) (d)

Fig. 3: The root GLR for $L = 200$ (a), and the estimated SCG waveforms in the x (b), y (c), and z (d) directions.

REFERENCES

[1] J. M. Zanetti and D. M. Salerno, "Seismocardiography: a technique for recording precordial acceleration," in *Proc. 4th Annual IEEE Symposium on Computer-Based Medical Systems*, (Baltimore, MD), pp. 4–9, May 12-14, 1991.

[2] J. M. Zanetti, M. O. Poliac, and R. S. Crow, "Seismocardiography: waveform identification and noise analysis," in *Proc. IEEE Conf. Computers in Cardiology*, (Venice , Italy), pp. 49–52, Sept. 23-26, 1991.

[3] R. A. Wilson, V. S. Bamrah, J. Lindsay, M. Schwaiger, and J. Morganroth, "Diagnostic accuracy of seismocardiography compared with electrocardiography for the anatomic and physiologic diagnosis of coronary artery disease during exercise testing," *The American Journal of Cardiology.*, vol. 71, pp. 536–545, Mar. 1993.

[4] A. Koch, P. McCormack, A. Schwanecke, P. Schnoor, C. Buslaps, K. Tetzlaff, and H. Rieckert, "Noninvasive myocardial contractility monitoring with seismocardiography during simulated dives," *Undersea and Hyperbaric Medical Society, Inc.*, vol. 30, pp. 19–27, 2003.

[5] Z.Trefny, K. Hana, S. Trojan, V. Toman, S. Herczegh, L. Pousek, and J. Slavicek, "New trends in balistocardiography," *Measurement Science Review*, vol. 3, Sec. 2, pp. 45–48, 2003.

[6] A. Dinh, Y. Choi, and S.-B. Ko, "A heart rate sensor based on seismocardiography for vital sign monitoring systems," in *Proc. 24th IEEE Canadian Conf. Electrical and Computer Engineering*, (Niagara Falls, Canada), pp. 665–668, May 8-11, 2011.

[7] A. Dinh, "Heart activity monitoring on smartphone," in *Proc. IEEE Int. Conf. Biomedical Engineering and Technol.*, vol. 11, (Singapore), pp. 45–49, 2011.

[8] P. Castiglioni, A. Faini, G. Parati, and M. D. Rienzo, "Wearable seismocardiography," in *Proc. IEEE EMBS Conf.*, (Lyon, France), pp. 3954–3957, Aug. 23-26, 2007.

[9] B. Ngai, K. Tavakolian, A. Akhbardeh, A. P. Blaber, K. B, and A. Noordergraaf, "Comparative analysis of seismocardiogram waves with the ultra-low frequency ballistocardiogram," in *Proc. IEEE EMBS Conf.*, pp. 2851–2854, Sept. 2-6, 2009.

[10] W. Sandham, D. Hamilton, A. Fisher, W. Xu, and M. Conway, "Multiresolution wavelet decomposition of the seismocardiogram," *IEEE Trans. Sig. Processing.*, vol. 46, pp. 2541–2543, Sept. 1998.

[11] M. Jerosch-Herold, J. Zanetti, H. Merkle, L. Poliac, H. Huang, A. Mansoor, F. Zhao, and N. Wilke, "The seismocardiogram as magnetic-field-compatible alternative to the electrocardiogram for cardiac stress monitoring," in *Int. Journal Cardiac Imaging*, vol. 15, pp. 523–531, Dec. 1999.

[12] K. Naemura and H. Iseki, "Damper design for improving S/N ratio of the seismocardiogram monitoring in the OpenMRI-guided operating theater," in *Proc. IEEE EMBS Conf.*, (San Francisco, CA), pp. 3428–3431, Sept. 2004.

[13] P. Smrcka, M. Jirina, Z. Trefny, and K. Hana, "New methods for precise detection of systolic complexes in the signal acquired from quantitative seismocardiograph," in *Proc. IEEE Int. Workshop on Intelligent Signal Processing*, pp. 375–380, Sept. 1-3, 2005.